Atmospheric Transport of Patagonian Dust and It's Influence on Marine Biological Activity in the South Atlantic Ocean

Matthew Johnson[1], Santiago Gassó[2], Nicholas Meskhidze[1], Fabien Solmon[3]

[1]North Carolina State University, Raleigh, NC, [2]Goddard Earth Sciences and Technology Center, [3]Laboratoire d'Aérologie, CNRS, Université de Toulouse, France

The global chemistry transport model GEOS-Chem, implemented with an iron dissolution scheme, was used in the analysis of Patagonian dust transport and the possible influence its deposition may have on marine biological activity. This study uses the combination of modeling and remote sensing techniques to analyze the horizontal and vertical structure of a large dust event on January 23, 2009. It was found that the transport dynamics such as synoptic meteorological patterns and associated storm strengths in the South Atlantic Ocean are the controlling factors in the downwind mineral dust transport. Through the comparison of remotely sensed data from Moderate Resolution Imaging Spectroradiometer (MODIS) and Cloud-Aerosol Lidar and Infrared Pathfinder Satellite (CALIPSO) with GEOS-Chem predicted dust burden, it was shown that the model could reasonably reproduce the transport of Patagonian dust over the South Atlantic Ocean. By applying the model predicted dust and dissolved iron fluxes to a phytoplankton bloom assessment model it was found that this dust event was unlikely to be sufficient in supplying enough bioavaliable iron to induce a phytoplankton bloom. However, sensitivity studies show that increases in mineral dust concentrations by a factor of 5 could possibly result in elevated levels of marine primary productivity in the surface waters of the South Atlantic Ocean.

1. Introduction

In many regions of the world's oceans (~30%) surface waters are defined by marine primary productivity that is limited by the micronutrient iron (Fe). There are three main high nitrate low chlorophyll (HNLC) oceanic regions (subarctic north Pacific, equatorial Pacific, and the Southern Ocean) and the Southern Ocean (SO) is suggested to be the most biogeochemically significant. The SO has said to be most important due to its large spatial extent and considerable influence on the global nutrient cycle [Sarmiento et al., 2004]. Fluxuations in the supply of Fe to the surface waters of the SO may play a key role in regulating biological productivity, atmospheric carbon dioxide (CO_2) concentration, and climate [Martin and Fitzwater, 1988; Martin et al., 1990; Zhuang et al., 1992; Jickells et al., 2005]. This potentially important role of Fe has lead to several artificial Fe experiments which have demonstrated the increase in phytoplankton primary productivity and increases in CO_2 drawdown following large additions of soluble Fe species [de Barrs et al., 2008; Pollard et al., 2009]. While artificial Fe experiments in the SO display noticeable influences on chlorophyll production it has been shown that natural Fe fertilization processes are on the order of ~4 times more efficient in producing carbon sequestration [de Barrs et al., 2008]. Despite the potentially important role of dust laden-Fe on

primary productivity in the polar and sub-polar waters of the SO, few studies exist that can help in constraining the atmospheric mineral dust and dust-laden Fe fluxes to the HNLC waters of the Atlantic sector of the SO. Most importantly, Patagonia has been estimated to supply the majority (up to 90%) of aeolian-Fe deposited to the South Atlantic Ocean (SAO) [Gaiero et al., 2006]. Therefore, there is a great need for improved understanding of mineral dust and dust-laden Fe emissions from Patagonia, transport pathways, and deposition to the surface waters of the SAO.

One of the major natural pathways of Fe to the surface waters of the SO is from the atmospheric deposition of aeolian dust [Martin et al., 1990; Watson et al., 2000; Boyd et al., 2000]. In the South Atlantic sector of the SO a significant correlation was measured between mean dissolved Fe (DFe) concentrations, in the subsurface layer, in comparison to total atmospheric deposition of dust laden-Fe [Sarthou et al., 2003]. However, the influence that mineral dust has on biological activity in the surface waters of HNLC oceans is complicated by the fact that only soluble/bioavaliable speciation of Fe are available for biological uptake [Jickells et al., 2005]. Further complicating this subject is the fact that processes producing bioavaliable Fe within atmospheric aerosols are presently not fully understood. Atmospheric processing of mineral dust has been suggested to be a major contributor to the mobilization of Fe due to the wide ranges of Fe solubilities reported far from the source (0.01-80%) [Siefert et al., 1997; Baker et al., 2006], while soluble portions of Fe at the source region are shown to be low (~0.1%) [Fung et al., 2000; Hand et al., 2004]. Forms of Fe found at the source region (e.g. hematite (α-Fe_2O_3) and goethite (α-FeO(OH)) are highly insoluble in oceanic waters [Stumm and Morgan, 1996; Fung et al., 2000; Bonnet and Guieu, 2004; Jickells et al., 2005; Journet et al., 2008] therefore, it has been proposed that chemical processing (e.g. acid mobilization) of mineral aerosols during their atmospheric transport may increase the amount of bioavaliable Fe in mineral dust [Duce and Tindale, 1991; Zhu et al., 1993; 1997; Meskhidze et al., 2003; 2005].

In this work we use the global chemistry transport model GEOS-Chem, implemented with a prognostic dust-Fe dissolution scheme (GEOS-Chem/DFeS model) [Solmon et al., 2009], to evaluate the transport pathways of Patagonian dust and deposition to the SAO. The magnitude and transport pathway of mineral dust from Patagonia to the SAO and Antarctica are presently highly misunderstood. This study will provide an in-depth analysis, using model and remotely sensed data, to better understand these transport pathways and assess the ability of GEOS-Chem to reproduce them. A second focus will be on quantifying the impact that Patagonian dust and DFe deposition has on the marine primary productivity in the mixed layer of the SAO surface waters. GEOS-Chem/DFeS will be used to simulate a large dust event in Patagonia which demonstrated large dust emissions and mineral dust transport over the SAO starting on January 23, 2009. Mineral dust and DFe deposition to the SAO will be quantified for this time period and implemented into a simple assessment tool of marine biological activity (described in section 2.2) to classify whether individual dust storms have the capability to induce phytoplankton blooms.

2. Methods

2.1 GEOS-Chem/DFeS

The three dimensional global chemistry transport model GEOS-Chem (v8-01-01) was used during this study to simulate mineral dust mobilization in Patagonia, transport, and

deposition to the surface waters of the SAO. The model uses GEOS-5 meteorological fields [Bey et al., 2001; Park et al., 2004; Evans and Jacob, 2005] at a 2° x 2.5° (latitude-longitude) grid resolution and 47 vertical levels. Importantly for the prognostic calculations of Fe dissolution, the model can be run with a full chemistry configuration. In its full chemistry configuration, GEOS-Chem includes H_2SO_4-HNO_3-NH_3 aerosol thermodynamics coupled to an O_3-NO_x-hydrocarbon-aerosol chemical mechanism [Bey et al.; 2001; Park et al., 2004]. Sulfur compounds, carbonaceous aerosols, and sea-salt emission and chemistry are accounted for and described by Park et al. [2004], Heald et al. [2004], and Alexander et al. [2005]. To simulate dust mobilization GEOS-Chem uses the Dust Entrainment and Deposition (DEAD) scheme [Zender et al., 2003]. Once mineral dust is mobilized from the surface the model uses four standard dust bins, with diameter boundaries of 0.2, 2.0, 3.2, 6.0 and 12 μm [Fairlie et al., 2007], to calculate and visualize global dust transport. Deposition processes (both wet and dry) are also simulated using the four individual dust bins [Fairlie et al., 2007]. GEOS-Chem has previously been shown to capture much of the amplitude and seasonal cycle in dust climatology at the surface sites of the North Pacific Ocean [Fairlie et al., 2007]. However, this research proved to be the first application of GEOS-Chem focusing on South American dust source regions, with a concentration on the deserts of Patagonia, and atmospheric transport processes leading to deposition in the SAO.

A prognostic, physically based dust-Fe dissolution module (DFeS) of Meskhidze et al. [2005] was previously implemented into GEOS-Chem (v7-03-06) [Solmon et al., 2009]. The DFeS model explicitly considers mineralogical composition of windblown dust and uses aqueous phase equilibrium and dissolution/precipitation reactions for the following minerals contained in dust: calcite, albite, microcline, illite, smectite, gypsum, and hematite [Meskhidze et al. 2005; Solmon et al., 2009]. The initial mineralogy prescribed to the model was developed to represent the transportable fraction (i.e., the fraction of the particles within desert top soils that can be uplifted and transported over large distances by wind) of Patagonian top soils. Nine key minerals that impact the pH of the deliquesced aerosol solution or influence the concentration of soluble Fe formed during atmospheric transport were chosen for the model simulations. Limited samples of Patagonian top soils have shown that clay minerals, quartz, and plagioclase are the main components likely available for uplift [Ramsperger et al., 1998; Smith et al., 2003; Gaiero et al., 2004]. The dissolution/precipitation of each mineral is estimated based on solution pH, temperature, dust mineralogy, and the specific surface area of the individual minerals. With prescribed mineralogical composition of dust and specified Fe content of minerals, DFeS can determine the amount of soluble Fe produced during atmospheric transport and transformation of mineral aerosols due to acidic attack (acid mobilization). It has previously been shown that GEOS-Chem/DFeS predicted fluxes of mineral dust and soluble Fe to the subarctic North Pacific Ocean were in reasonable agreement with available observational data [Solmon et al., 2009].

2.2 Marine Biology Assessment Tool

A simple assessment tool was previously developed by Boyd et al. [2009] to determine the possibility that an individual dust storm could initiate a phytoplankton bloom in regions of Fe starved surface waters. This tool is not a predictive model but a set of equations (spreadsheet form) that sets upper and lower limits on variables, which are widely misunderstood, that link dust and DFe deposition with phytoplankton growth. These equations are described in detail in Boyd et al. [2009] and have been adjusted during this study to allow focus on the SAO and

permit the linkage to GEOS-Chem/DFeS. For example, the initial assessment tool was designed to calculate dust deposition according to the "half-decrease distance" formula [Prospero et al., 1989]. However during this study, we have altered equations to allow GEOS-Chem predicted mineral dust deposition fluxes to be used in the assessment tool. Another improvement made during this study is GEOS-Chem/DFeS was applied to calculate DFe deposition, while in the original equations an a priori and constant portion of total dust was considered to be soluble. By using GEOS-Chem/DFeS we can produce more realistic and variable amounts of DFe within dust produced by ambient environmental conditions without defining an initial and constant dissolved Fe fraction (DIF).

A second part to the assessment module calculates the change in DFe concentrations in the mixed layer due to atmospheric dust and DFe deposition, biological uptake, and horizontal and vertical particulate export fluxes. During this study it is assumed that a phytoplankton bloom can be induced if DFe concentrations exceed a predetermined threshold for an assigned time period. Boyd et al. [2009] demonstrated this technique is most sensitive to the initial DFe concentration in the surface waters, DIF (here considered to be the fraction of total Fe within dust that is dissolved/soluble), leachable fraction of Fe, rate of biological uptake of Fe, lifetime of Fe within the mixing layer, and the half-decrease distance for dust deposition. The assumptions made for these variables and used during baseline simulations are shown in Table 1.

Table 1 Variables and their assigned values for the baseline simulations of dust/biota responses demonstrated during this study.

Tool Input Variable	Value	Data Sources
Mixed Layer (m)	65	Boyd and Law, 2001
$[Fe_{Background}]$ (pM d^{-1})	0.004	Bowie et al., 2001
$[Fe_{Initial}]$ (nM)	0.12	Moore and Braucher, 2007
Fe_{dust}%	3.5	Duce and Tindale, 1991
DFe_{dust}%	GEOS-Chem	
$Fe_{leachable}$%	30	Mackie et al., 2006
$Rate_{leachable}$ (d^{-1})	30	Frew et al., 2006
$[FeExport_{inorganic}]$ (pM d^{-1})	6	Bowie et al., 2001
$[FeExport_{organic}]$ (pM d^{-1})	3	Bowie et al., 2001
Uptake t=0 (pM d^{-1})	3	Bowie et al., 2001
$[DFe]_{threshold}$ (nM)	0.2	de Barrs et al., 2008
$Time_{threshold}$ (days)	4	Boyd et al., 2009

2.3 Satellite Data

Due to the limitation in model evaluation produced by the severe deficit of in-situ measurements of dust fluxes and concentrations in Patagonia and the SAO, we must use remotely sensed data to fill the gaps. To evaluate mineral dust transport predicted by GEOS-Chem we compare calculated daily averaged dust burden to Level 2 and 3 aerosol optical depths (AOD @ 550nm) obtained from the Moderate Resolution Imaging Spectroradiometer (MODIS) [Salomonson et al., 1989; King et al., 1996]. Specifically by using the "Fraser Method" [Fraser et al., 1984], similar to the methodology demonstrated in Gassó and Hegg, [2003], we were able to derive columnar aerosol mass concentrations (AMC) from MODIS AOD. Using both MODIS AOD and AMC we could evaluate the model predicted magnitude and the spatial distribution of daily averaged mineral dust burden. The reason why this method can be used over Patagonia,

and specifically over the SAO, is due to the pristine nature of this region. The major aerosols in this region can be assumed to be largely made up of dust and sea-salt particles. To justify comparing total AMC to dust burden we analyzed the percent mass of mineral dust compared to sea salt within Patagonian dust plumes during the January 23, 2009 dust event. It was found (data not shown here) that mineral dust was the dominant (>80%) contributor to total mass in the areas of largest dust transport.

With an assumption that single scattering albedo (SSA (ω_o)) and mass scattering efficiency (mse (α_{sp})) are constant throughout the atmospheric column; the equation below was applied to calculate AMC (g m^{-2}) with the only variable being AOD (τ_{ext}):

$$m_{col} = \frac{\omega_o \times \tau_{ext}}{\alpha_{sp}}$$

During this study the SSA and mse are set to represent mineral dust at 0.8 ± 0.2 [Ostrum and Noone, 2000] and 0.4 ± 0.3 m^2 g^{-1} [Carlson and Caverly, 1977] respectively. By using the above constants, representative of dust aerosols, we can confidently compare MODIS AMC with model predicted dust burden in areas of maximum mineral dust transport. During this study MODIS Deep-Blue algorithms were not applied due to the focus of dust transport taking place over the dark surfaces of the SAO. Final MODIS AOD values were derived from averaging both Terra and Aqua (instantaneous) land and ocean measurements to increase spatial coverage and produce a more reasonable comparison to model predicted daily averaged dust burden.

The Cloud-Aerosol Lidar and Infrared Pathfinder Satellite Observation (CALIPSO) Cloud-Aerosol Lidar with Orthogonal Polarization (CALIOP) instrument was used during this study to analyze the vertical profile of mineral dust transport over the SAO. This instrument derives vertical profiles of attenuated backscatter at 532 and 1064 nm during both day and night portions of the satellites orbit. The CALIOP laser emits two beams of linearly polarized light and is composed of a telescope which collects the backscattered light produced by molecules and particles at each level of the atmosphere [Winker et al., 2007]. The intensity of the backscattered attenuated signal depends on the aerosol vertical distribution while the depolarization ratio is related to their shape. In addition to total backscatter at both wavelengths, CALIOP provides profiles of linear depolarization at 532 nm. The depolarization measurement enables discrimination between ice and water clouds and identification of non-spherical (dust) aerosol particles. During this research the CALIPSO Level 1 data products (version 2.02) are used exclusively and contain the cloud and aerosol layer and column properties. Patagonian dust aerosols can be identified at a given altitude range of the vertical profiles through the analysis of attenuated backscatter and depolarization profiles at 532 nm. The dust depolarization ratio is high because of the non-spherical nature of mineral dust particles. This differs from most other particles which are spherical and have a depolarization ratio of near zero values. Therefore, the depolarization ratio is normally used as an indicator to separate dust from other aerosol types [Murayama et al., 2001].

3. Results

3.1 Mineral Dust Emissions and Atmospheric Transport

3.1.1 Dust Emission

In order to evaluate mineral dust transport over the SAO a combination of model predicted daily dust concentrations compared to that derived from remotely sensed data proved to be the best method to fully capture transport pathways. Firstly, to understand mineral dust transport we wanted to identify how well GEOS-Chem captures individual dust outbreaks in Patagonia. To do this we chose to focus on a large dust storm that occurred on January 23, 2009. The reason why this event was chosen was due to clear images of dust advection remotely sensed by MODIS (Figure 1) and CALIPSO sensors. This is important because comparisons of model predicted dust source regions and transport pathways with remotely sensed data from Patagonia is difficult, as the dust plumes over the SAO have been shown to travel at low altitudes and are generally accompanied by large amounts of cloud cover [Gassó and Stein, 2007]. Clear imagery captured by both Aqua and Terra would allow for the analysis of how GEOS-Chem captured the dust emission source and initial atmospheric transport.

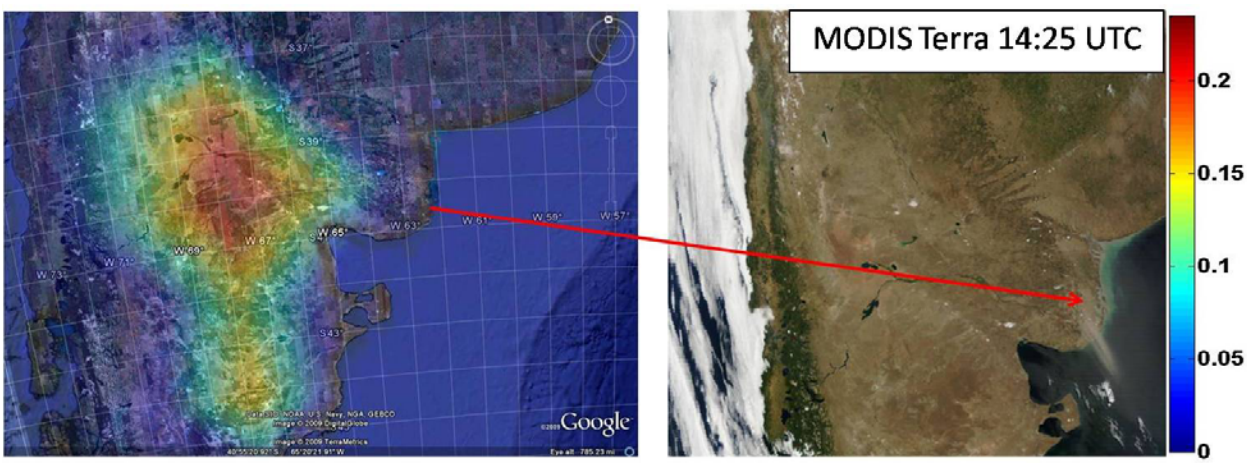

Figure 1 GEOS-Chem predicted daily total dust emissions on January 23, 2009 (Tg day^{-1}). This image illustrates model predicted dust emissions overlaid on Google Earth topography maps compared to MODIS Terra remotely sensed real-time imagery for this day. The red arrow indicates the error in the spatial distribution of mineral dust mobilization predicted by GEOS-Chem in comparison to remotely sensed data.

Figure 1 illustrates GEOS-Chem predicted dust emissions in Patagonia on January 23, 2009 compared to that remotely sensed by MODIS Terra satellites. Both Terra and Aqua real-time imagery captured the dust plume out of Patagonia on this day, however we focus on Terra (morning pass) due to the dust source becoming active during the morning hours. Seen in Figure 1 GEOS-Chem does not produce dust emission regions in compliance with that seen from MODIS real-time imagery. By overlaying GEOS-Chem predicted dust emissions over Google Earth topography maps it was found that the model produces dust emission regions located ~4.5 to 5.0˚ west of that seen during the MODIS Terra overpass. This modeling error produces dust advection originating from a region located ~500 to 550 km west compared to what actually occurred. Due to the large dust storm producing maximum dust emissions over 0.2 Tg, this could potentially have a profound influence on the location and magnitude of dust deposition in

the SAO. The fact that such a large quantity of dust was emitted (an order of magnitude larger than the monthly average) from an incorrect dust source led us to evaluate how modeling errors during dust emissions can influence downwind mineral dust transport.

While GEOS-Chem did prove to accurately capture the timing of the large dust event that occurred on January 23, 2009, the model produced emissions regions inaccurately. A likely reason why the model produces emission regions much further from the coast than that observed by MODIS satellites is due to the large grid resolution used by GEOS-Chem. The DEAD scheme calculates whether a grid cell is a candidate for dust mobilization by the following land characteristic variables: dry land fraction, bare ground fraction, land surface type, surface temperature, and vegetative area index [Zender et al., 2003]. The model calculates emissions on a 2˚x2.5˚ grid scale which may not allow the model to produce small dust emission regions such as that seen during this dust event. The most important variable to consider here is a model grid cell must be greater than 50% dry land with little to no vegetative cover to be even considered for dust mobilization in the DEAD scheme. As seen from Figure 1 the dust emission region was located on the coast of Patagonia which will most likely not be considered a potential grid cell for dust mobilization. Another importance fact to consider is the large drought conditions that have gripped the flat lands of Patagonia during this time period. Point sources for this dust plumes appear to have originated in the agricultural region north of Golfo San Matías, which has been said to be the region worst affected by the present drought conditions. Such recent and drastic land characteristic changes may not be well represented by the input files initiating the GEOS-Chem model.

3.1.2 Mineral Dust Transport

It has been shown that the dominant atmospheric wind pattern over Patagonia and the SAO is predominantly from the west [Paruelo et al., 1998]. However, previous studies [i.e. Li et al., 2008] have shown that Patagonia is the dominant source of mineral dust to the eastern portion of Antarctica. This section will analyze the factors influencing both west to east and north to south transport of mineral dust over the SAO. During this study it was observed that the transport pathway of mineral dust out of Patagonia is highly dependent on the synoptic patterns of storm systems in the SAO and Southern Ocean. Through the evaluation of dust burden spatial patterns and sea-level pressure (SLP) anomalies it is seen that the positioning and strength of high and low pressure systems (determined by pressure gradient (SLP anomaly)) control the path and advection speed of dust transport. Figure 2 demonstrates how the synoptic setup of SLP anomalies produce the path and advection speed of dust advected during the January 23, 2009 dust storm. From this figure it can clearly be seen that dust follows the pathway in which opposing pressure systems are adjacent and synoptic flows produce winds in similar directions. This channeling affect produced by high pressure systems being present to the east of low pressure systems seems to be the dominant pathway of dust reaching Antarctica. This analysis demonstrates the importance of the location of high and low pressure systems to the southward transport of mineral dust over the SAO.

Through additional analysis it was also found that the strength and number of high and low pressure systems are directly correlated with dust concentrations over the eastern sector of Antarctica. A study was conducted by initializing two separate simulations with constant mineral dust concentrations over Patagonia and the SAO. The two separate simulation time periods November 1-10, 2008 (simulation A) and December 24, 2008 through January 2, 2009

(simulation B) were chosen due to similar synoptic patterns; however simulation A proved to have noticeably stronger SLP anomalies when compared to simulation B. To make sure that the differences between the two simulations was only due to storm strength, dust emissions were shut off to ensure that storm strength did not influence the magnitude of dust present over the SAO. By separating SLP anomalies (SLPA) into 3 separate categories of calm (SLPA < 10 mb), moderate (10 mb < SLPA < 20 mb), and strong (SLPA > 20 mb) we could decipher how storm intensity influenced dust transport over Antarctica. For both simulations (A and B) a strong positive correlation was found between storm strength and southward dust transport over Antarctica with correlation coefficients of 0.60 and 0.55 respectively. This point was even further emphasized through calculations of total dust that was transported to Antarctica in each separate simulation. Simulation A presented 71% more grid points corresponding to moderate or strong storm conditions and produced 32% more dust over Antarctica when compared to simulation B. This study shows preliminary results that the strength along with the positioning of synoptic patterns is directly correlated with the timing, location, and magnitude of dust transported southward over Antarctica.

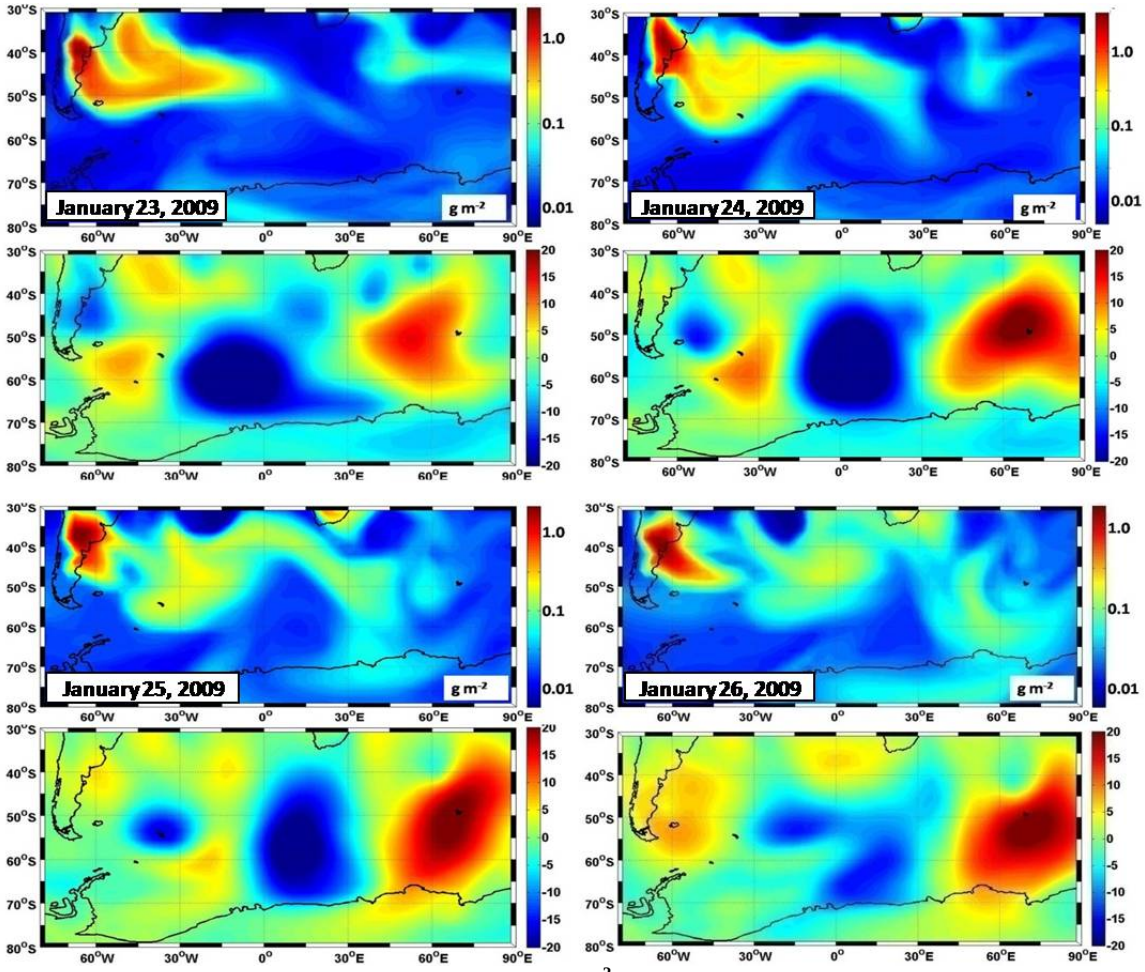

Figure 2 GEOS-Chem predicted daily dust burden (g m^{-2}) compared to SLP anomalies over the SAO during the time period of January 23-26, 2009. These images illustrate the dependence of mineral dust transport on the spatial location of SLP anomalies. Cold colors indicate negative SLP anomalies (low pressure systems) and warm colors display high pressure systems.

To evaluate the GEOS-Chem predicted transport pathway of mineral dust advected on January 23, 2009, we use MODIS AOD to calculate AMC in comparison with model simulated daily averaged dust burden. Figure 3 displays how model predicted dust concentrations compare to that derived from MODIS satellite retrievals on the first day of emissions. From this figure it can be seen that the model predicted dust burdens are within an order of magnitude of aerosol concentrations calculated from MODIS AOD. It is important to focus on the areas in which mineral dust is present; the large under estimations south of 56°S are due to sea salt aerosols not being considered by GEOS-Chem during this study. While column dust concentrations and MODIS AMC are in general agreement there seems to be slight difference in the trajectory of the main dust plume present on January 23, 2009. In Figure 3 it can be seen that the model demonstrates an overestimation of dust burden to the west of what was captured by MODIS and an underestimation around 0 to 0.6 g m^{-2} (black circle in Fig. 3) in the location of actual dust transport captured by MODIS. The path predicted by the model is similar in shape but due to being emitted from an incorrect source, ~5° to the west of what was seen by MODIS, aerosol concentrations compared to dust burdens are slightly inconsistent. This study demonstrates the importance of dust emission location on that accuracies of simulating initial (first day) dust transport out of Patagonia.

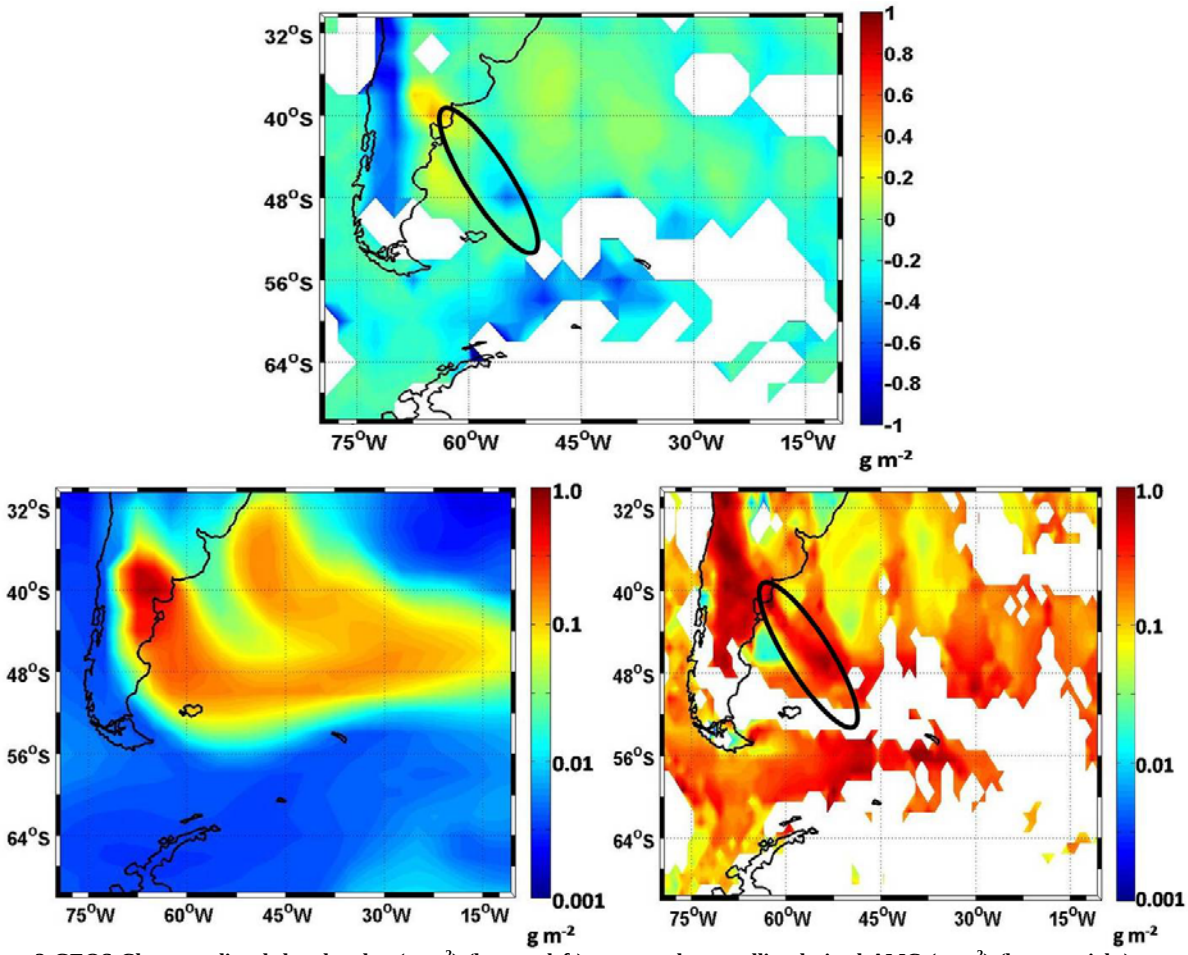

Figure 3 GEOS-Chem predicted dust burden (g m^{-2}) (bottom left) compared to satellite derived AMC (g m^{-2}) (bottom right) over the SAO on January 23, 2009. The difference between model predicted concentrations (top) shows the model calculated dust within an order of magnitude to that seen from MODIS. The satellite derived main dust transport pathway is highlighted by a black circle and indicates a spatial error in initial model predicted dust transport on this day.

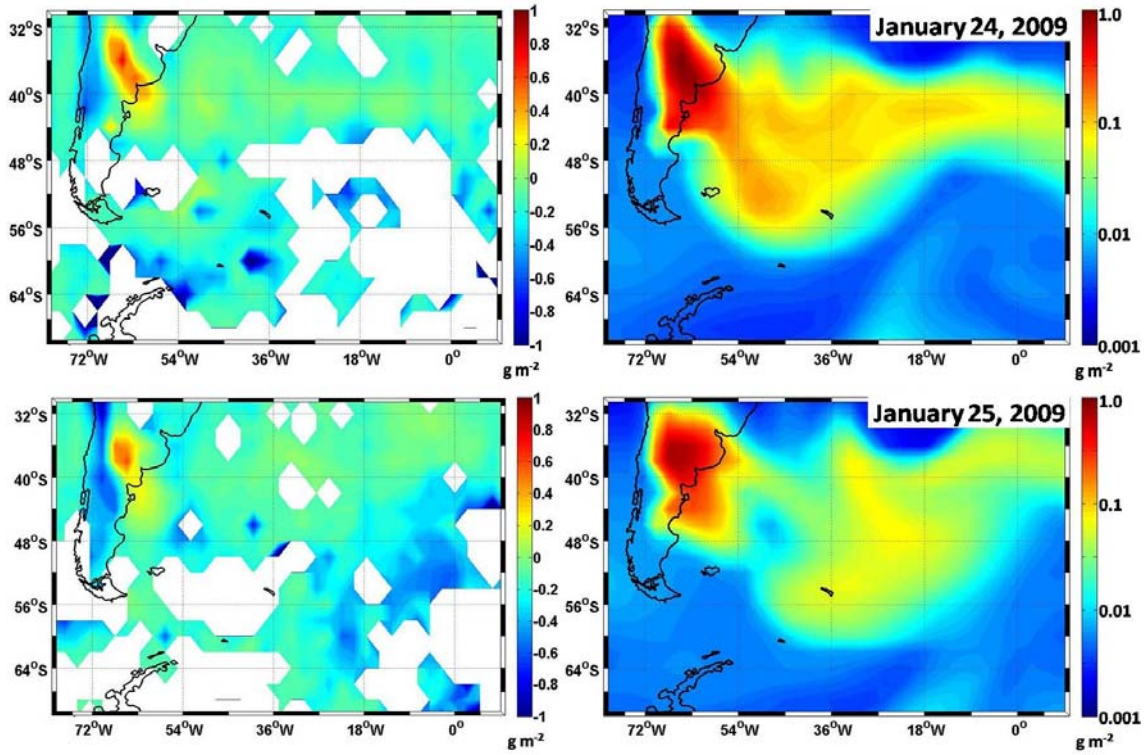

Figure 4 GEOS-Chem predicted dust burden (g m^{-2}) (right) and the difference between model predicted dust concentrations and MODIS AMC (left) for January 24, 2009 (top) and January 25, 2009 (bottom).

To evaluate the model's ability to simulate the downwind transport of the advected dust we perform the same analysis as that conducted for January 23, 2009 for the two preceding days. Only the two preceding days were analyzed due to mineral dust concentrations becoming small enough that remotely sensed data demonstrated no indication that dust was present. Figure 4 illustrate how the model predicted dust burden compares to AMC calculated with MODIS AOD for Jan. 24 and Jan. 25, 2009. Focusing on the areas of the main dust transport you can see the model predicted dust burden begins to become more consistent with MODIS AMC as the plume progresses. While the increase in accuracies are small on January 25, 2009 the model predicts dust concentrations on average ~0.015 g m^{-2} closer in agreement with MODIS AMC in the region of dust transport (between 35°S-60°S and 50°W-10°E) when compared to January 24, 2009. This suggests a possible uncoupled relationship between downwind dust concentration and spatial distribution and the exact location of dust emissions. This fact was further evaluated using the HYbrid Single-Particle Lagrangian Integrated Trajectory (HYSPLIT) model to evaluate how dust is transported from the emission point predicted by GEOS-Chem and the emission point seen by MODIS real-time imagery. Figure 5 demonstrates aerosol concentrations at 6z for January 23 and 0z for January 24-26, 2009 for runs with separate emission points and a combined emission point simulation. Demonstrated in this figure is the fact that regardless of emission point location, plume trajectories will become identical downwind from Patagonia over the SAO. The plumes become so similar that separate spatial representation, disregarding differences in concentrations, in comparison with MODIS AOD demonstrates little to no differences. These exercises have demonstrated that downwind transport of mineral dust is independent of exact emission sources and is mainly controlled by transport dynamics and synoptic weather patterns.

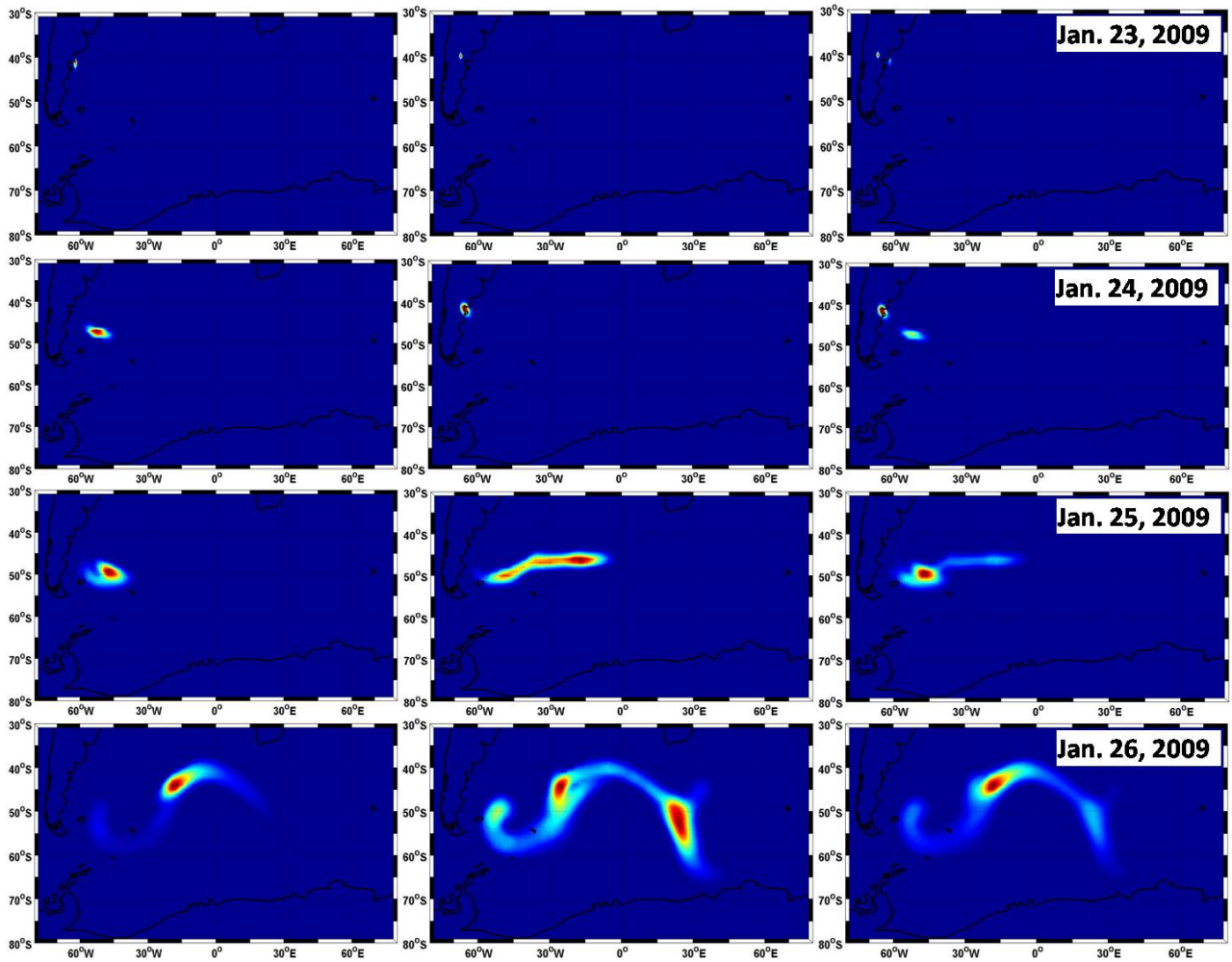

Figure 5 HYSPLIT aerosol transport displaying dust transport path for dust emitted from the source captured by MODIS real-time imagery (left), GEOS-Chem predictions (middle), and both (right).

A similar result was discovered by Colarco and Toon, [2003] which illustrated that mineral dust transport far downwind of the Sahara desert is largely uncoupled from the timing of emissions and is more dominantly influence by transport dynamics. This study used modeling and in-situ AOD measurements to demonstrate this uncoupling. However, due to the lack of ground-based measurements of aerosols or AOD downwind of Patagonia we will rely on GEOS-Chem predicted dust transport to understand if this fact is true for dust emitted in the deserts of Patagonia. To simulate differences in emission timing, two individual simulations were conducted allowing mineral dust to be mobilized only on January 22 and January 23, 2009 separately. Figure 6 illustrates a similar discovery that was demonstrated in Colarco and Toon, [2003] as downwind mineral dust transport pathways are very similar for the separate simulations. It is apparent in this figure that dust reaches the Antarctic coast on the same day (Jan. 26, 2009) regardless of the day of emissions. While concentrations reaching the coast of Antarctica on this day are slightly higher for the simulation presenting dust emissions one day earlier, these concentrations will become closer in magnitude the further downwind dust is transported. From these studies it can be seen that locations and timing of dust emission in Patagonia has a large initial influence on mineral dust transport during the day of emissions. However, these studies have shown that downwind from the source the dominant process

controlling dust transport pathways are transport dynamics such as the synoptic setup and strength of high and low pressure systems.

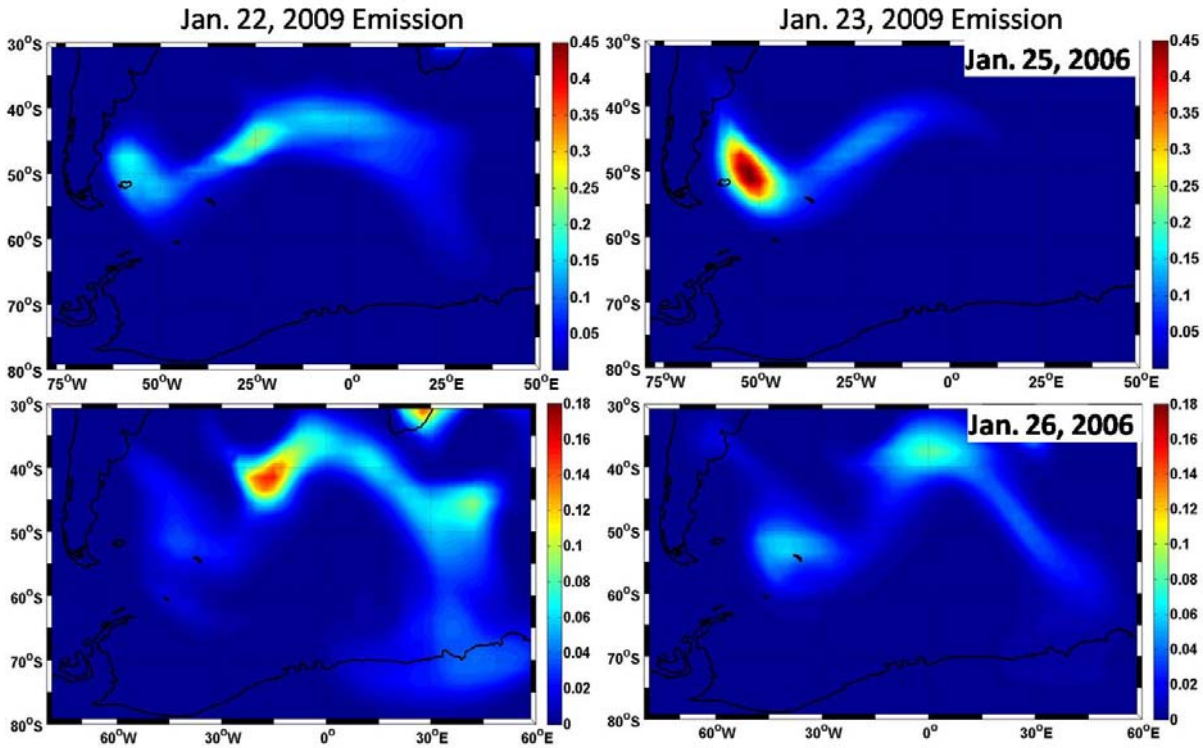

Figure 6 GEOS-Chem predicted dust burden (g m^{-2}) on January 25 (top) and January 26, 2009 (bottom) for dust emitted only on January 22 (left column) and January 23, 2009 (right column). This figure shows how regardless of emission timing Patagonian dust plumes take similar shapes dominantly determined by transport dynamics.

For the analysis of the vertical structure of the dust plume advected on January 23, 2009 we chose to compare longitudinally averaged cross-sections of GEOS-Chem predicted dust concentrations and CALIPSO satellite retrievals. Figure 7a and 7b illustrate vertical profiles of aerosols derived from CALIPSO and vertical cross-sections of dust concentrations predicted by GEOS-Chem for Jan. 23-24, 2009. These days were focused on due to clear images captured by CALIPSO, which over the SAO proves difficult caused by large cloud presence. Through the analysis of model predicted dust plume heights and CALIPSO data it was found that GEOS-Chem correctly produces vertical profiles of mineral dust during this outbreak. Interestingly from the vertical profiles of dust produced by the model and remotely sensed data you can further see the importance of pressure systems in the vertical distribution of dust over the SAO. In Figure 7b, on January 24 it can clearly be seen that the dust is being advected vertically in the atmosphere as the dust plume becomes encompassed within a low pressure system. From the CALIPSO over pass on January 24, 2009 between 45.2°S, 44°W and ~55°S, 49°W you can see a profound lifting. Comparing this same transect to weather maps (not shown here) and the SLP anomalies illustrated in Figure 2 on January 24, 2009 it can be seen this lifting is directly associated with the advection into a low pressure system**.** This part of the research further demonstrates the importance of low pressure systems in the transport of Patagonian dust plumes.

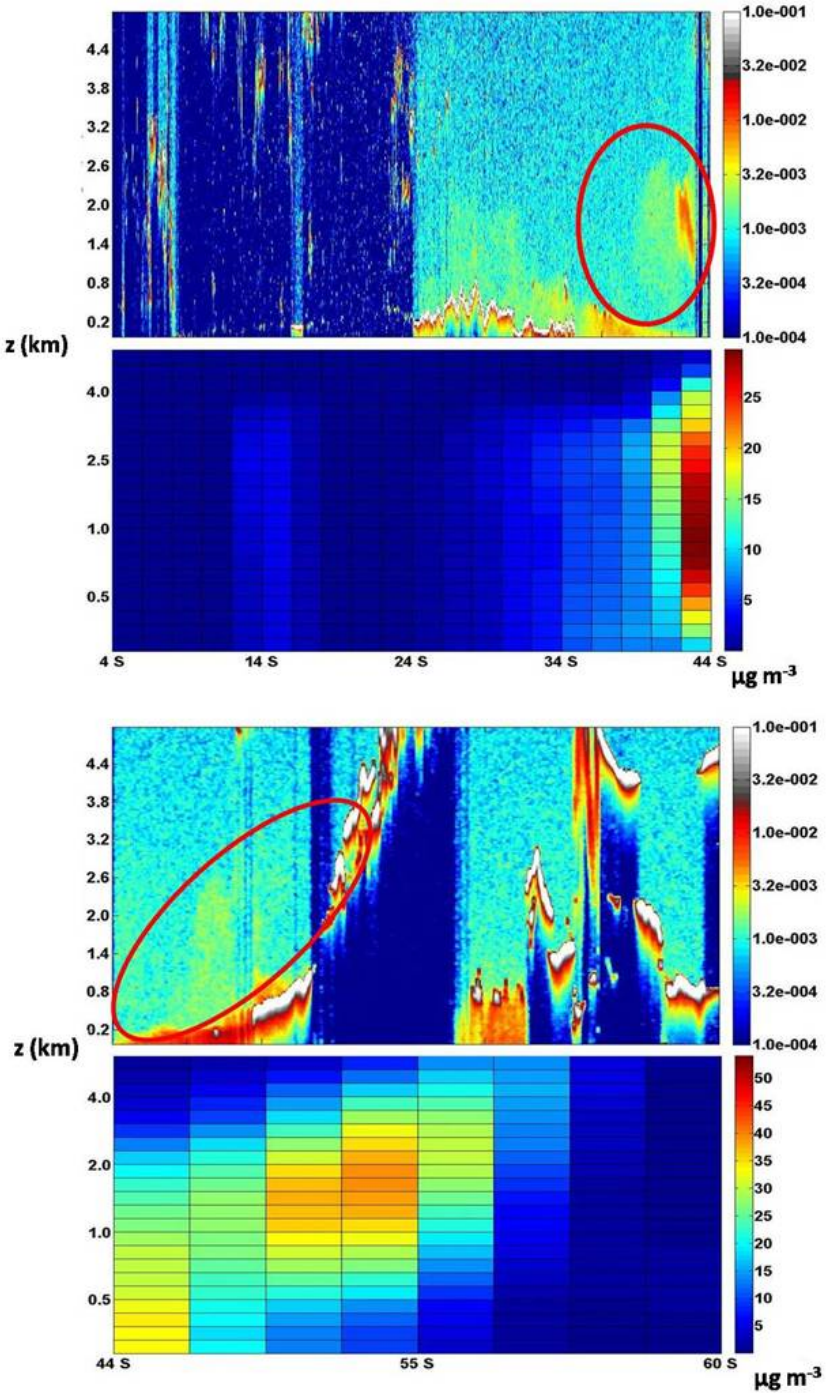

Figure 7 CALIPSO attenuated backscatter (552nm) compared to GEOS-Chem predicted dust concentrations on a) January 23, 2009 (top) and b) January 24, 2009 (bottom). The red circles indicate aerosols displaying elevated depolarization ratios which are characteristic of mineral dust. We then could compare these regions of dust capture by CALIPSO to vertical cross-sections of predicted dust concentrations from GEOS-Chem.

This study has already demonstrated that the horizontal dust transport over the SAO is most likely controlled by the location and strength of high and low pressure systems. It also seems that the vertical structure of Patagonian dust plumes are most likely produced by lifting induced by convergence associated with low pressure systems over the SAO. In this section we

wished to evaluate the extent of elevation to which dust plumes are transported as they reach the Antarctic coastline. Figure 8 shows the horizontal and vertical structure of mineral dust on January 26, 2009 (4 days after emission) that was emitted on January 23, 2009. This figure shows that when the dust emitted from Patagonia reached the coast of Antarctica it had been elevated to ~7-9km. While it has been shown in previous studies [i.e. Li et al., 2008] that dust transported from Patagonian tends to remain within the boundary layer, this study shows that dust associated with strong low pressure systems can reach levels of high elevation necessary for long range transport. This exact process is shown on the 50°S vertical cross-section demonstrated in Figure 8. As the Patagonian dust plume enters the western side of the large low pressure (~40°W) maximum dust concentrations are located 1-2 km above the SAO. As the dust plume is advected clockwise around the large low pressure system to the eastern portion of the anti-cyclone (~30°E) the dust has been elevated to ~8 km above the surface.

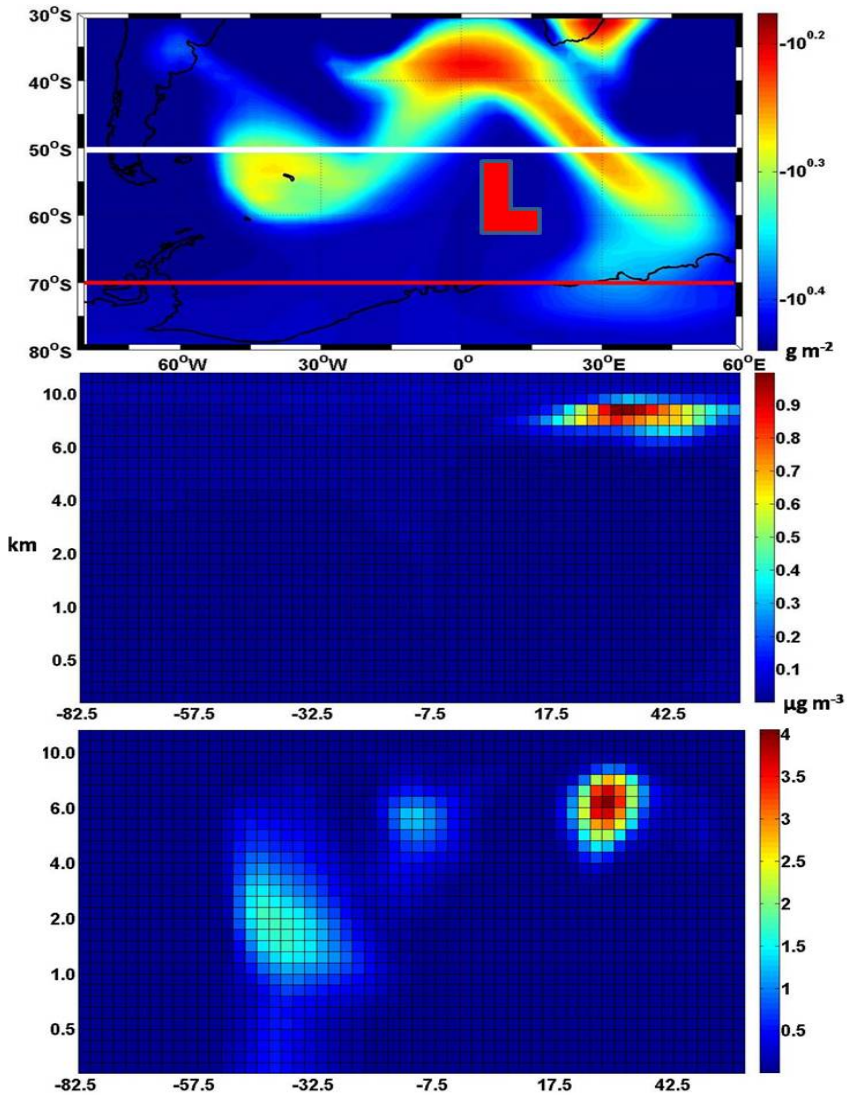

Figure 8 GEOS-Chem predicted dust burden (g m^{-2}) (top) and vertical cross-sections of dust concentrations (µg m^{-3}) averaged at 70°S (middle) shown by the red line and the white line indicates the transect at 50°S (bottom) on January 26, 2009.

3.2 Dust and DFe Deposition

With confidence that our model has a general handle on the transport of the dust advected on Jan. 23, 2009, we then could insert predicted dust and DFe deposition fluxes to the phytoplankton bloom assessment tool. From Figure 9 it can be seen that substantial amounts of dust was deposited to the SAO during the dust event with areas receiving fluxes up to 10,000 µg m^{-2} day^{-1}. However it can also be seen from this figure that the mineral dust deposited to the SAO displayed low DIF. Low DIF calculated in Patagonian dust during this time period would limit the amount of bioavaliable Fe supplied from the initial deposition of mineral dust. An important aspect of this research is that we have the ability to assess the influence of the atmospheric and biological production of soluble Fe. While limited DFe production from acid mobilization is evident from Figure 9, large amounts of dust will still be available for longer term oceanic dissolution process such as: grazer/particle interaction [Hutchins and Bruland, 1994], photo-reductive processes during interactions with marine siderophores [Kraemer et al., 2005], and the reduction of mineral Fe within particle micro-zones. The focus during this study is predominantly on the bioavaliable Fe supplied from atmospheric deposition and its impact on marine primary productivity (assessed in section 3.3). An in-depth analysis of long term dissolution processes using the marine phytoplankton assessment sheet is demonstrated in Boyd et al. [2009].

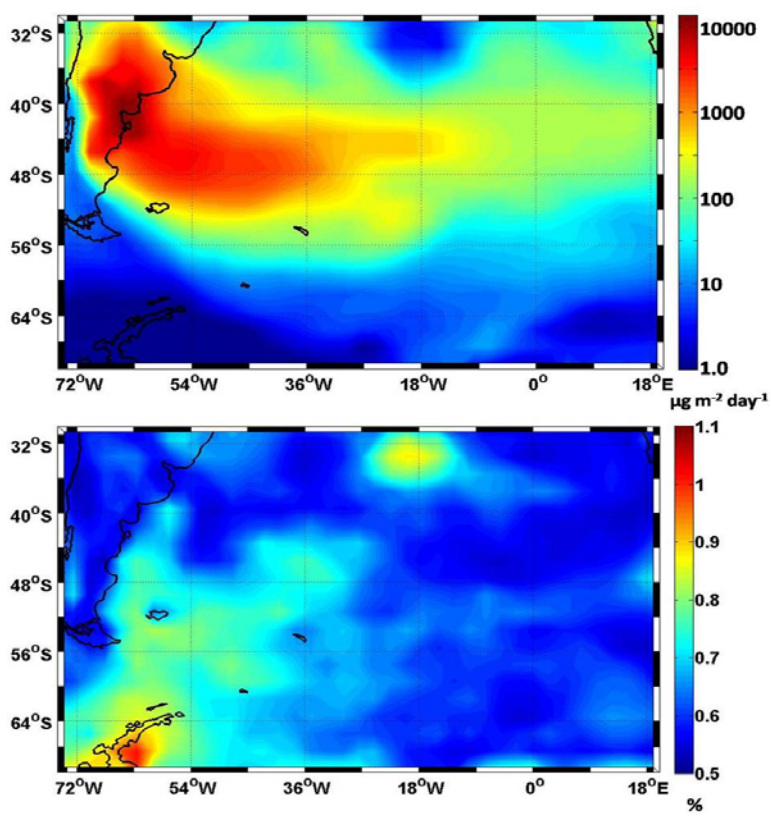

Figure 9 GEOS-Chem predicted average daily dust deposition (µg m^{-2} day^{-1}) to the SAO (top) and average DIF of dust deposited (right) between Jan. 23-30, 2009.

Dust deposited to the SAO surface waters, during the time period of January 23-39, 2009, displayed DIF ranging between 1.1% and 0.46%. The inferred values of DIF over the SAO domain are significantly less than ones found downwind from east Asia [Solmon et al., 2009], using a previous version of GEOS-Chem/DFeS, and are thought to be primarily attributed to low concentration of anthropogenic acidic trace gases available to be mixed with Patagonian dust. Considering that initial DIF of Patagonian soil was initially prescribed in the Fe dissolution scheme to be 0.45%, such low DIF values suggest that acid mobilization may not be the important mechanism for producing dissolved Fe in the SAO domain. Substantial acidification of aeolian dust, prior to its deposition to the ocean, may be required to solubilize the large fraction of mineral dust laden-Fe present during large dust outbreaks in order to produce bioavaliable Fe. However, these results are consistent with our earlier studies based on remote sensing data analysis in the Atlantic sector of the SO suggesting that dust deposition may not be the controlling mechanism for biological activity in this region [Meskhidze et al., 2007].

3.3 Marine Primary Productivity Response to Mineral Dust Deposition

Using GEOS-Chem calculated dust and DFe deposition fluxes we could then determine whether the Patagonian dust event on Jan. 23, 2009 was likely to initiate increased marine primary productivity in the Fe-limited waters in the SAO below the Subtropical Front (~40°S). To ensure any oceanic primary productivity was induced by atmospheric dust deposition we would only study areas greater than 500km off the coast of South America to negate upwelling of Fe rich waters from below. To determine if this dust event had the capability to induce phytoplankton growth, daily dust and DFe depositions between 45-51°S and 49-56°W (area corresponding to large daily dust deposition (Fig. 9) in Fe-limited waters during dust event) were implemented into the marine phytoplankton assessment sheet. The threshold for the concentration of DFe necessary to be present in the mixed layer in order to induce a phytoplankton boom was chosen to be 0.2 nM for at least 4 consecutive days [de Barrs et al., 2008]. The study by de Barrs et al. [2008] stated that during the Southern Ocean Iron Enrichment Experiment DFe concentrations inside blooms of diatoms were always above ~0.2 nM. Figure 11 illustrates DFe concentrations present in the area of interest between Jan. 23-29, 2009 produced by daily Patagonian dust and DFe depositions. From this figure it can be seen that the dust and associated DFe deposited during the dust outbreak is most likely to be insufficient in producing a phytoplankton bloom.

Our modeling results for the contribution of mineral dust to the total Fe budget is consistent with previous oceanographic studies, suggesting that aeolian input is likely to account for less than 10% of DFe concentration in the surface waters of the NPO. However, our modeling result also show, that distribution of DIF as well as total dissolved Fe fluxes can be very complex and highly variable in both space and time. Therefore, prescription of constant DIF for atmospheric input of continental dust, as were often done in the previous assessments, may lead to incorrect estimates for the role of aeolian dust in different regions of the SAO. While dust plumes may not commonly deposit sufficient quantities of bioavaliable Fe to cause visible blooms (typically less than 10%, [Blain et al., 2007; Wagener et al., 2008]), episodic supply of dissolved Fe from Patagonia may still be important source of micronutrient Fe for HNLC waters of the SAO. Detailed analyses of hydrographic data concurrently with in-situ studies of mineral dust composition and soluble Fe fraction may be necessary to unambiguously identify the role of Patagonian dust for biological productivity in the SAO.

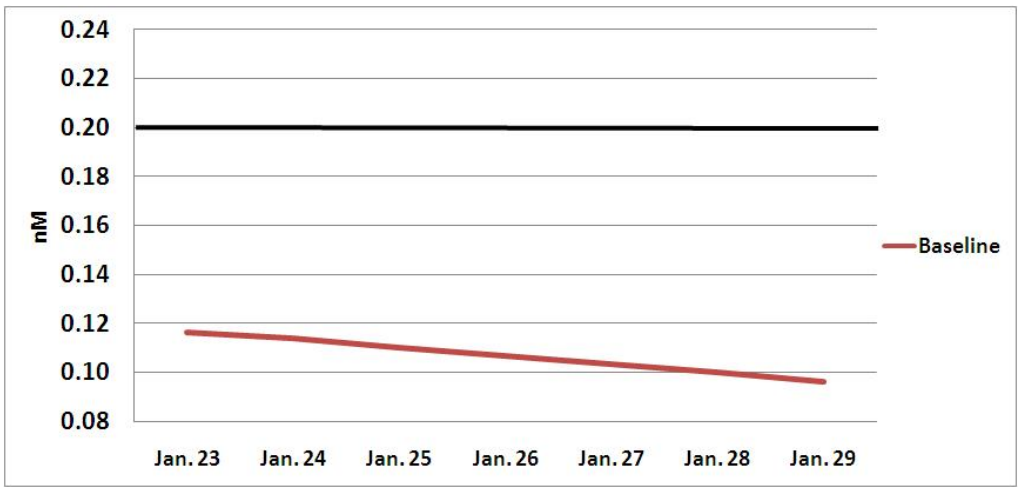

Figure 11 DFe concentrations (nM) present in the SAO surface waters (red line) due to dust and DFe depositions between January 23-29, 2009. The black line indicates the threshold of DFe needed to induce a phytoplankton bloom in this region.

While the dust storm of January 23, 2009 proved unlikely to have supplied sufficient bioavaliable Fe to the surface waters of the SAO to induce a phytoplankton bloom, there were larger dust events that occurred during the austral winter of 2008-2009. To narrow down case studies in which to focus we ran daily correlations in the SAO between SeaWiFS satellite derived chlorophyll *a* concentrations and GEOS-Chem predicted dust deposition rates between November 2008 and February 2009. While monthly averaged and seasonality of dust deposition and surface chlorophyll concentrations in the SAO have been shown to be positively correlated, there are significant variation in the temporal pattern of blooms, spatial extent, and strength that cannot be accounted for by the variation in mineral dust [Meskhidze et al., 2007]. This point was evident when conducting the analysis of the daily variations in dust deposition and SAO during this study. No large positive correlations were found (using a 0-10 day delay between dust deposition and chlorophyll concentrations) except during the dust events occurring in February 2009 and particularly that one simulated by GEOS-Chem starting on February 11, 2009. Figure 12 demonstrates mixed layer DFe concentrations, calculated in the phytoplankton assessment sheet, present during this dust deposition event. It can be seen from this figure that while baseline dust and DFe depositions were not enough to induce phytoplankton growth it could counteract biological uptake and horizontal and vertical transport (apparent from the constant oceanic DFe concentrations). The fact this storm may have been able to support phytoplankton populations already present in the area led us to wonder what variables and conditions would need to be present to actual produce a phytoplankton bloom during this dust event.

Due to the uncertainty in variables used in calculating DFe concentrations in the surface waters of the SAO and model predicted aerosol concentrations, we chose to conduct a sensitivity study using variable mineral dust concentrations. This sensitivity study conducted would involve increasing dust and DFe deposition rates in accordance to the differences seen between GEOS-Chem predicted dust concentrations and MODIS AMC within the January 23, 2009 dust plume. Discussed previously GEOS-Chem proved to predicted mineral dust concentrations within an order of magnitude in comparison with MODIS AMC. However in certain areas this could lead to column dust burdens that are factor of 10 less than that seen from remotely sensed data. To test whether these potential errors could influence phytoplankton growth we increased

dust deposition rates by a factor of 5 and 10. Seen from Figure 12, increasing deposition by a factor of 5 and 10 both led to bioavaliable Fe concentrations exceeding the set threshold (0.2 nM) for more than 4 days which theoretically could produce a phytoplankton bloom. This case study demonstrates a good case study for deeper analysis as daily dust deposition during this time period had strong positive correlation coefficients (0.32-0.64 for 0 to 8 day time lags) not seen in other time periods between November 2008 and February 2009.

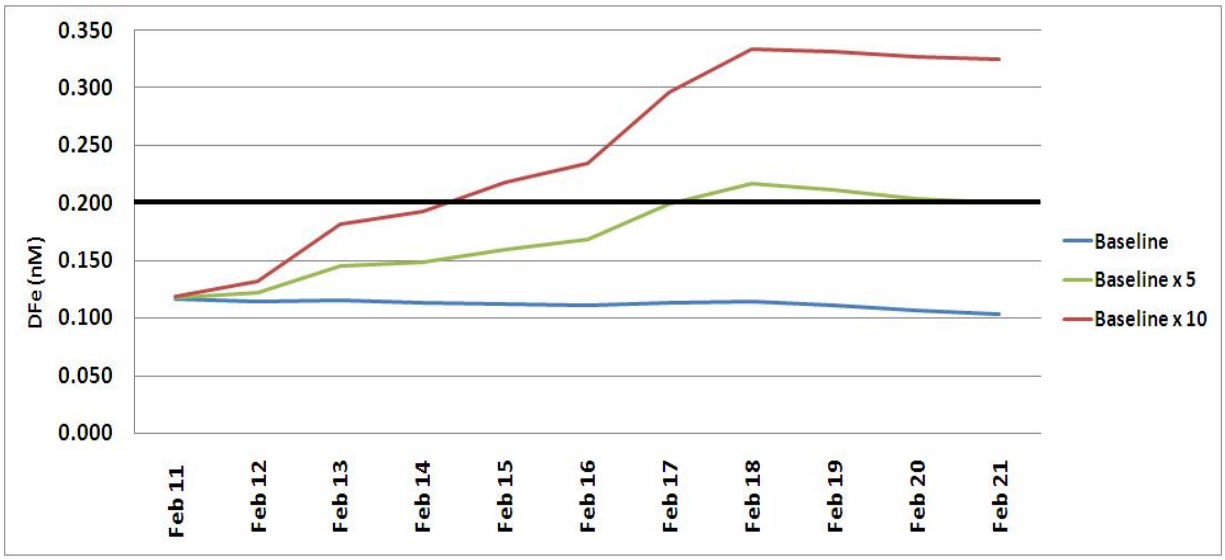

Figure 12 Cumulative [DFe] predicted from the dust/biota assessment tool during the dust event of February 11, 2009. Baseline [DFe] (blue line) shows that mineral dust and DFe depositions were sufficient and sustaining oceanic bioavaliable Fe concentrations. However when increasing deposition fluxes by a factor of 5 (green line) and 10 (red line) [DFe] exceed the predetermined threshold in order to potentially induce a phytoplankton bloom.

4. Conclusions

Despite the potential importance of the atmospheric Fe supply to the SO from dust sources in the Southern Hemisphere, only a few studies have been conducted to analyze dust transport for this region [Genthon, 1992, Krinner and Genthon, 2003, Gassó and Stein, 2007; Li et al., 2008]. This study was conducted to better understand the dominant processes that define transport pathways of dust advected from the deserts of Patagonia. Another important aspect of this study was to better understand whether individual dust outbreaks in Patagonia could supply bioavaliable Fe supplies sufficient enough to initiate phytoplankton blooms in the HNLC oceans of the SAO. In this study, the global chemistry transport model GEOS-Chem, implemented with a prognostic Fe dissolution scheme, was applied to the SAO during the January 23, 2009 dust event to analyze model predicted dust transport. A focus of this research was to use modeling techniques in combination with remotely sensed data to assist in the analysis along with evaluating the models ability to reproduce the dust transport out of Patagonia.

While the general air mass trajectory and wind directions over Patagonia and the SAO are dominantly from west to east [Paruelo et al., 1998], southward dust advection towards Antarctica is evident. This led to the interest of how does dust come to reach the southward extent of the Southern Hemisphere (below 70°S), specifically in the South Atlantic sector of the

SO, and to the eastern portion of the continent of Antarctica. In this study it was shown that the dominate factor controlling dust transport out of Patagonia and over the SAO is the synoptic setup and strength of the storms present in the region. The transport dynamics displayed by the synoptic meteorology over the SAO not only controlled horizontal transport pathways but vertical structure also. It has previously been shown that the majority of Patagonian dust remains mostly in the boundary layer and is not available for long-range transport. However, during this study it was shown that strong low pressure systems over the SAO advect dust vertically up to ~9 km by the time dust reaches the coast of Antarctica. This fact shows that these strong anti-cyclones may be necessary for Patagonian dust to be transported over long distance. Along with the finding that synoptic patterns and storm strength are the controlling factor of the downwind dust transport over the SAO, it was also found that GEOS-Chem demonstrates the capability to reasonably reproduce this complex dust transport. This was shown through the comparisons of horizontal and vertical structure of model predicted dust transport with remotely sensed data from MODIS and CALIPSO. The ability for models to accurately reproduce mineral dust transport in this region is important due to low dust concentrations and high cloud coverage making the usage of remote sensing difficult [Gassó and Stein, 2007]. These results were shown through the methodology of combining and comparing modeling and remotely sensed data during the dust event initiated on January 23, 2009.

During this study, GEOS-Chem simulated dust and DFe depositions were implemented into a marine phytoplankton bloom assessment sheet to see if this event could support a phytoplankton bloom. The model predicted elevated amounts of dust were deposited to the SAO surface waters up to a week after emissions (10,000 $\mu g\ m^{-2}\ day^{-1}$), however due the pristine nature of the Patagonian region the prognostic Fe dissolution scheme predicted low DIF present at the time of dust deposition. This finding further shows that acid mobilization may not be the dominant process in producing bioavaliable Fe in dust aerosols over the SAO due to the limited concentrations of acidic traces being insufficient to initiate large scale Fe mobilization. The dust event of January 23, 2009 proved unlikely to supply enough bioavaliable Fe to induce a phytoplankton bloom or any large scale marine primary productivity increases. These findings further support the idea that atmospheric deposition of Fe may not be the controlling factor of phytoplankton production in the surface waters of the SO.

To study larger dust deposition events, a simulated dust outbreak beginning on February 11, 2009 was then studied to determine what conditions were needed to actually induce a phytoplankton bloom in the SAO. Baseline deposition fluxes of both mineral dust and DFe for this event proved to keep oceanic DFe concentrations constant, counteracting that taken up by phytoplankton and horizontal and vertical transport. Sensitivity studies, encouraged by specific areas of possible underestimation of mineral dust concentrations, demonstrated that a factor of 5 or 10 increases in mineral dust and DFe concentrations could possibly have induced a bloom. This finding illustrates the need for global transport models to accurately represent not only the magnitude but transport pathway of mineral dust to fully understand the influence that atmospheric aerosol depositions can have on marine primary productivity.

Overall, during this research it was shown that the combination of modeling and remotely sensed data is an important methodology in order to understand the atmospheric transport of Patagonian dust over the SAO. This methodology allowed for not only the analysis of mineral dust transport over the SAO but also model evaluation of the global chemistry transport model GEOS-Chem. Having confidence in aerosol transport models in this region is necessary due to dust concentrations tending to be too small to be remotely sensed and dust plumes are often

masked by cloud cover. Further knowledge of the transport and deposition of mineral dust and dust laden bioavaliable Fe is needed to further the understanding of the relationship between atmospheric aerosols and oceanic primary productivity. With further insight gained from studies similar to the one presented here, a better understanding of important topics in science such as oceanic carbon sequestration and dust activity coupling with past and future climate change can be achieved.

References

Alexander, B., J. Savarino, C. C. W. Lee, R. J. Park, D. J. Jacob, M.H. Thiemens, Q. B. Li, R. M. Yantosca (2005), Sulfate formation in sea-salt aerosols: Constraints from oxygen isotopes, *J. Geophys. Res.*, *110*, D10307.

Baker, A. R., T. D. Jickells, M. Witt, and K. L. Linge (2006), Trends in the solubility of iron, aluminium, manganese and phosphorus in aerosol collected over the Atlantic Ocean, *Mar. Chem., 98,* 43-58.

Blain et al. (2007), Effect of natural iron fertilization on carbon sequestration in the Southern Ocean. *Nature. 446*, doi: 10.1038/nature05700.

Bey, I., et al. (2001), Global modeling of tropospheric chemistry with assimilated meteorology: model description and evaluation. *J. Geophys. Res*., *106*, 23073–23096.

Bonnet, S., and C. Guieu (2004), Dissolution of atmospheric iron in seawater, *Geophys. Res. Lett., 31*, doi:10.1029/2003GL018423.

Bowie, A. R., M. T. Maldonado, R. D. Frew, P. L. Croot, E. P. Achterberg, R. F. C. Mantoura, P. J. Worsfold, C. S. Law, and P. W. Boyd (2001), The fate of added iron during a mesoscale fertilization experiment in the Southern Ocean, *Deep-Sea Res., 48,* 2703-2743.

Boyd et al. (2000), A mesoscale phytoplankton bloom in the polar Southern Ocean stimulated by iron fertilization, *Nature, 407*, 695-702.

Carlson, T. N., and R. S. Caverly (1977), Radiative characteristics of Saharan dust at solar wavelengths, *J. Geophys. Res., 82*, 3141-3152.

Colarco, P. R., et al., Saharan dust transport to the Caribbean during PRIDE: 2. Transport, vertical profiles, and deposition

in simulations of in situ and remote sensing observations, *J. Geophys. Res., 108*, 8590, doi:10.1029/2002JD002659, 2003.

Boyd, P. W., D. S. Mackie, and K. A. Hunter (2009), Aerosol iron deposition to the surface ocean: Modes of iron supply and biological responses, doi:10.1016/j.marchem.2009.01.008.

Boyd, P. W., and C. S. Law (2001), The Southern Ocean Iron Release Experiment (SOIREE): introduction and summary, *Deep-Sea Res., 48,* 2425-2438.

de Barr, H. J. W., L. J. A. Gerringa, P. Laan, and K. R. Timmermans (2008), Efficiency of carbon removal per added iron in ocean iron fertilization, *Mar. Ecol. Prog. Ser., 364,* 269-282.

Duce, R. A., and N. W. Tindale (1991), Atmospheric transport of iron and its deposition in the ocean, *Limnol.Oceanogr., 36*, 1715-1726.

Evans, M. J., and D. J. Jacob (2005), Impact of new laboratory studies of N2O5 hydrolysis on global model budgets of tropospheric nitrogen oxides, ozone, and OH, *Geophys. Res. Lett., 32*, L09813, doi:10.1029/2005GL022469.

Fairlie, T. D., J. Jacobs, and R. J. Rokjin (2006), The impact of transpacific transport of mineral dust in the United States, *Atmos. Env.., 41*, 1251–1266.

Fairlie, T. D., M. A. Avery, R. B. Pierce, J. Al-Saadi, J. Dibb, and G. Sachse (2007), Impact of multiscale dynamical processes and mixing on the chemical composition of the upper troposphere and lower stratosphere during the Intercontinental Chemical Transport Experiment–North America, *J. Geophys. Res.*, *112*, doi:10.1029/2006JD007923.

Frew, R. D., D. A. Hutchins, S. Nodder, S. Sanudo-Wilhelmy, A. Tovar-Sanchez, K. Leblanc, E. Hare, P. W. Boyd (2006), Particulate iron dynamics during FeCycle in subantarctic waters southeast of New Zealand, *Global Biogeochemical Cycles, 20.*

Fung, I. Y., S. K. Meyu, I. Tegen, S. C. Doney, J. G. John, and J. K. B. Bishop (2000), Iron supply and demand in the upper ocean. *Global Biogeochem. Cycles, 14,* 281–295.

Gaiero, D. M., J. L. Probst, P. J. Depetris, S. M. Bidart, and L. Leleyter (2004), Iron and other transition metals in Patagonian riverborne and windborne materials: Geochemical control and transport to the southern Atlantic Ocean, *Geochimica et Cosmochimica Acta, 67*, 3603-3623, doi: 10.1016/S0016-7037(03)00211-4.

Gaiero, D. M., F. Brunet, J. L. Probst, and P. J. Depetris (2006), A uniform isotopic and chemical signature of dust exported from Patagonia: Rock sources and occurrence in southern environments, *Chem. Geo., 238*, 107-120, doi: 10.1016/j.chemgeo.2006.11.003.

Gasso´, S., and D. A. Hegg, On the retrieval of columnar aerosol mass and CCN concentration by MODIS, *J. Geophys. Res., 108*, 4010, doi:10.1029/2002JD002382, 2003.

Gasso´, S., and A. F. Stein (2007), Does dust from Patagonia reach the sub-Antarctic Atlantic Ocean?, Geophys. Res. Lett., 34, L01801, doi:10.1029/2006GL027693.

Genthon, C. (1992), Simulations of desert dust and sea salt aerosols in Antarctica with a general circulation model of the atmosphere, *Tellus, Ser. B, 44,* 371-389.

Hand, J. L., N. M. Mahowald, Y. Chen, R. L. Siefert, C. Luo, A. Subramaniam, and I. Fung (2004), Estimates of atmospheric-processed soluble iron from observations and a global mineral aerosol model: Biogeochemical implications, *J. Geophys. Res., 109*, D17205, doi:10.1029/2004JD004574.

Heald, C. L., D. J. Jacob, D. B. A. Jones, P. I. Palmer, J. A. Logan, D. G. Streets, G. W. Sachse, J. C. Gille, R. N. Hoffman, and T. Nehrkorn (2004), Comparative inverse analysis of satellite (MOPITT) and aircraft (TRACE-P) observations to estimate Asian sources of carbon monoxide, *J. Geophys. Res., 109*, D23306, doi:10.1029/2004JD005185.

Hutchins, D. A., and K. W Bruland (1994), Grazer-mediated regeneration and assimilation of Fe, Zn and Mn from planktonic prey. *Mar. Eco. Prog. Ser., 110*, 259–269.

Jickells et al. (2005), Global Iron Connections Between Desert Dust, Ocean Biogeochemistry, and Climate, *Science*, *308*, 67-71.

Journet, E., K. V. Desboeufs, S. Caquineau, and J.-L. Colin (2008), Mineralogy as a critical factor of dust iron solubility, *Geophys. Res. Lett., 35*, doi:10.1029/2007GL031589.

King, et al. (1996), Airborne scanning spectrometer for remote sensing of cloud, aerosol, water vapor, and surface properties, *J. Atmos. Oceanic Technol., 13*, 777–794.

Kraemer, S. M., A. Butler, P. Borer, and J. Cervini-Silva (2005), Siderophores and the dissolution of iron-bearing minerals in marine systems. Molecular Geomicrobiology. Reviews in Mineralogy & Geochemistry. Mineralogical Soc America, Chantilly, pg. 53–84.

Krinner, G., and C. Genthon (2003), Tropospheric transport of continental tracers towards Antarctica under varying climatic conditions, *Tellus, 55B,* 54-70.

Li, F., P. Ginoux, and V. Ramaswamy (2008), Distribution, transport, and deposition of mineral dust in the Southern Ocean and Antarctica: Contribution of major sources, *J. Geophys. Res*., *113*, doi: 10.1029/2007JD009190.

Mackie, D. S., P. W. Boyd, G. H. McTainsh, N. W. Tindale, T. K. Westberry, K. A. Hunter (2008), Biogeochemistry of iron in Australian dust: from eolian uplift to marine uptake. *Geochemistry Geophysics Geosystems, 9*.

Martin, J. H. (1990), Glacial-Interglacial CO_2 Change: The Iron Hypothesis, *Paleoceanography*, *5*, 1–13.

Martin, J. H., and S. E. Fitzwater (1988), Iron-deficiency limits phytoplankton growth in the northeast pacific subarctic, *Nature*, *331*, 341-343.

Meskhidze, N., W. L. Chameides, A. Nenes, and G. Chen (2003), Iron mobilization in mineral dust: Can anthropogenic SO_2 emissions affect ocean productivity?, *Geophys. Res. Lett., 30*, doi:10.1029/ 2003GL018035.

Meskhidze, N., W. L. Chameides, and A. Nenes (2005), Dust and pollution: A recipe for enhanced ocean fertilization?, *J. Geophys. Res., 110*, D03301, doi: 10.1029/2004JD005082.

Meskhidze, N., A. Nenes, W. L. Chameides, C. Luo, and N. Mahowald (2007), Atlantic Southern Ocean productivity: Fertilization from above or below?, *Global Biogeochem. Cycles*, *21*, GB2006, doi: 10.1029/2006GB002711.

Moore, J. K., and O. Braucher (2007), Observations of dissolved iron concentrations in the World Ocean: implications and constraints for ocean biogeochemical models, *Biogeosciences Discuss., 4,* 1241-1277.

Murayama, et al. (2001), Ground-based network observations of Asian dust events of April 1998 in east Asia, *J. Geophys. Res., 106*, 18,345-18,359.

Ostrom, E., and K. J. Noone (2000), Vertical profiles of aerosol scattering and absorption measured in situ during the North Atlantic Aerosol Characterization Experiment (ACE-2), *Tellus, Ser. B, 52*, 526-545.

Park, R. J., D. J. Jacob, B. D. Field, R. M. Yantosca, and M. Chin (2004), Natural and transboundary pollution influences on sulfate-nitrate-ammonium aerosols in the United States: implications for policy, *J. Geophys. Res., 109*, doi: D15204, 10.1029/2003JD004473.

Pollard et al. (2009), Southern Ocean deep-water carbon export enhanced by natural iron fertilization, *Nature, 457,* 577-581.

Prospero, J. M., M. Uematsu, and D. Savoie (1989), Mineral aerosol transport to the Pacific Ocean, In: Riley, J.P., Chester, R., Duce, R. (Eds.), Chemical Oceanography. Academic Press, New York, pg. 187–218.

Ramsperger, B., N. Peinemann, and K. Stahr (1998), Deposition rates and characteristics of Aeolian dust in the semi-arid and sub-humid regions of the Argentinean Pampa, *J. of Arid Env., 39*, 467-476.

Salomonson, V. V., W. L. Barnes, P. W. Maymon, H. E. Montgomery, and H. Ostrow (1989), MODIS: Advanced facility instrument for studies of the Earth as a system, *IEE Trans. Geosci. Remote Sens., 27*, 145-153.

Sarmiento, J. L., N. Gruber, M. A. Brzezinski, and J. P. Dunne (2004), High latitude controls of the global nutricline and low latitude biological productivity, *Nature*, *427*, 56– 60.

Sarthou et al. (2003), Atmospheric iron deposition and sea-surface dissolved iron concentrations in the eastern Atlantic Ocean, *Deep-Sea Res., 50,* 1331-1352.

Siefert, R. L., A. M. Johansen, M. R. Hoffmann, and S. O. Pehkonen (1997), Measurements of trace metal (Fe, Cu, Mn, Cr) oxidation states in fog and stratus clouds, *J. Air Waste Manage. Assoc., 48*, 128– 143.

Smith, J., D. Vance, R. A. Kemp, C. Archer, P. Toms, M. King, and M. Zarate (2003), Isotopic constraints on the source of Argentinian loess with implications for atmospheric circulation and the provenance of Antarctic dust during recent glacial maxima. *Earth and Planetary Science Letters 212*, 181–196.

Solmon, F., P. Y. Chuang, N. Meskhidze, and Y. Chen (2009), Acidic processing of mineral dust iron by anthropogenic compounds over the north Pacific Ocean, *J. Geophys. Res., 114*, doi:10.1029/2008JD010417.

Stumm, W., and Morgan, J. J. (1996): Aquatic Chemistry, Chemical Equilibria and Rates in Natural Waters, 3rd ed. John Wiley & Sons, Inc., New York, pg. 1022.

Wagener, T., C. Guieu, R. Losno, S. Bonnet, and N. Mahowald (2008), Revisiting atmospheric dust export to the Southern Hemisphere ocean: Biogeochemical implications, *Global Biogeochem. Cycles,* 22, GB2006, doi:10.1029/2007GB002984.

Watson A. J., D. C. E. Bakker, A. J. Ridgwell, P. W. Boyd and C. S. Law (2000), Effect of iron supply on Southern Ocean CO_2 uptake and implications for glacial atmospheric CO_2, *Nature, 407*, 730–733.

Winker, D. M., W. H. Hunt, and M. J. McGill (2007), Initial performance assessment of CALIOP, *Geophys. Res. Lett., 34*, L19803, doi:10.1029/ 2007GL030135.

Zender, C. S., D. Newman, and O. Torres (2003), Spatial heterogeneity in aeolian erodibility: Uniform, topographic, geomorphic, and hydrologic hypotheses, *J. Geophys. Res*., *108*, doi: 10.1029/2002JD003039.

Zhu, X., J. M. Prospero, D. L. Savoie, F. J. Millero, R. G. Zika, and E. S. Saltzman (1993), Photoreduction of iron (III) in marine mineral aerosol solutions, *J. Geophys. Res., 98*, 9039–9046.

Zhu, X. R., J. M. Prospero, and F. J. Millero (1997), Diel variability of soluble Fe(II) and soluble total Fe in North African dust in the trade winds at Barbados, *J. Geophys. Res., 102*, 21,297–21,305.

Zhuang, G., Z. Yi, R. A. Duce, and P. R. Brown (1992), Link between iron and sulphur cycles suggested by detection of Fe(II) in remote marine aerosols, *Nature, 355*, 537–539.